Available online at www.sciencedirect.com
SCIENCE DIRECT®

Journal of the European Ceramic Society 23 (2003) 2323–2335
www.elsevier.com/locate/jeurceramsoc

Low temperature hydrothermal synthesis and formation mechanisms of lead titanate ($PbTiO_3$) particles using tetramethylammonium hydroxide: thermodynamic modelling and experimental verification

Seung-Beom Cho[a,*], Jun-Seok Noh[a], Malgorzata M. Lencka[b], Richard E. Riman[c]

[a]*Advanced Materials Research and Development, LG Chemical Ltd., Research Park, 104-1, Moonji-dong, Yusong-gu, Daejeon, 305-380, South Korea*
[b]*OLI System, Inc., 108 American Road, Morris Plains, NJ, USA*
[c]*Department of Ceramics, College of Engineering, Rutgers, The State University of New Jersey, Piscataway, NJ, USA*

Received 5 October 2002; received in revised form 3 January 2003; accepted 20 January 2003

Abstract

Thermodynamic modeling was used to predict the optimum synthesis conditions for precipitation of the phase-pure lead titanate ($PbTiO_3$) in the Pb–Ti-tetramethylammonium hydroxide (TMAH) system using a newly developed computer program for automatic generation of stability and yield diagrams. The thermodynamic model has been experimentally validated over a wide range of processing conditions. Like KOH-mineralized systems, it was determined that the pH of the hydrothermal reaction medium and the Pb/Ti ratio are critical factors in forming stoichiometric $PbTiO_3$ powder. Morphological evolution during the reaction suggests that the formation mechanism appears to be controlled by a dissolution and recrystallization process. Two possible growth mechanisms are proposed based on the magnitude of the Pb/Ti ratio. In the case of Pb/Ti ratio = 1.1, at the early stage of the reaction (3 h) excess lead species promote the formation of spherical intermediate pyrochlore phase followed by the formation of primary cubic $PbTiO_3$ crystals. The growth of cubic $PbTiO_3$ crystals proceeds until the intermediate phase acting as a reservoir to provide precipitating ions is consumed. In case of Pb/Ti ratio = 1.25, excess lead condition leads to the formation of a platelet-shaped intermediate pyrochlore phase. These platelet intermediate particles act as a template in which small cubic shaped $PbTiO_3$ grains grew on the surface of these platelets.

Keywords: Actuators; $PbTiO_3$; Platelets; Powders-chemical preparation; Thermodynamic modelling

1. Introduction

In recent years, there has been an increasing interest in the synthesis of monodispersed metal oxide particles with controlled morphology. Such particles are desired for a variety of applications including fabrication of ceramic-polymer composites for electronic applications and as a reinforcement phase in polymer and brittle matrix composites.[1–3]

Lead titanate ($PbTiO_3$) is an important ferroelectric material with a variety of applications, which involve multilayer capacitors, resonators, and ultrasonic transducers.[4]

Significant research has been conducted on the formation of $PbTiO_3$ via calcination routes using starting powders derived by mixed oxide,[5] sol-gel,[6] precipitation from homogeneous solution (PFHS),[7] or coprecipitation.[8] Sol-gel derived and coprecipitated powders are fine in size but a calcination/crystallization step is necessary, which introduces extensive particle aggregation.

Hydrothermal synthesis is a low temperature method for the direct preparation of anhydrous multicomponent crystalline ceramic powders.[3] Hydrothermal synthesis involves the treatment of aqueous solutions or suspensions of precursor materials at temperatures typically ranging from room temperature to 1000 °C and pressures ranging from atmospheric to 100 MPa. This method can produce fine, high purity, stoichiometric particles of single and multicomponent metal oxides. Furthermore, if process conditions such as solution pH,

* Corresponding author. Tel.: +822-866-2415; fax: +822-862-6069.
E-mail address: sebcho@lgchem.com (S.-B. Cho).

0955-2219/03/$ - see front matter © 2003 Elsevier Ltd. All rights reserved.
doi:10.1016/S0955-2219(03)00085-2

solute concentration, reaction temperature, reaction time, and the type of solvent are carefully controlled, ceramic particles of the desired shape and size can be produced.

Hydrothermal formation of lead titanate has been extensively studied, including the thermodynamic phase equilibria for lead titanate in water.[9–16] However, a successful hydrothermal synthesis where both phase and morphology are controlled requires the optimization of processing parameters that include temperature, precursor concentrations and pH. In most cases, this has been done by time consuming empirical trial and error method. To rationalize the design of a hydrothermal synthesis process, Lencka et al.[11,12,16] proposed a comprehensive thermodynamic model that simulates the behavior of heterogeneous systems containing solids and an aqueous phase with dissolved electrolytes. In all cases, KOH was used as a pH-adjusting agent. It has been reported however that powders precipitated form alkali-containing systems may be contaminated by alkalis and/or halides and alkali ion caused the hardening of PZT.[17] Most recently, this thermodynamic model has been used to predict processing conditions for the synthesis of the phase-pure $PbZr_{0.52}Ti_{0.48}O_3$ powders in alkali-free medium.[18]

Our research has some novel features different from the present technology. Choice of mineralizers is most important. Choices of mineralizers must be made on the basis that undesirable impurities should not be incorporated in the crystal and they should have a favorable effect on the growth habit of the crystal. In our research, TMAH was used as pH-adjusting agent (mineralizer) to prevent the contamination by alkalis and/or halides, which are commonly used in conventional hydrothermal process. The objective of the current research is to investigate the applicability of the model to alkali free systems by using TMAH. A newly developed computer program for thermodynamic modeling was used to investigate the optimum synthesis conditions in the Pb–Ti–TMAH–H_2O system. The thermodynamic model was validated experimentally over a wide range of processing conditions. Also, possible formation mechanisms of perovskite $PbTiO_3$ are proposed in the Pb–Ti–TMAH–H_2O system.

2. Thermodynamic modeling

2.1. Thermodynamic modeling of the Pb–Ti–TMAH–H_2O system

A thermodynamic model of electrolyte solutions[11,19] is used in this work to calculate phase equilibria in the Pb–Ti–H_2O system in the presence of an organic mineralizer (i.e., tetramethylammonium hydroxide). This model combines information about standard-state properties of all species that may exist in the hydrothermal system with a formulation for the excess Gibbs energy, which accounts for solution nonideality. The model has been successfully applied to the hydrothermal synthesis of various perovskite-type materials.[12,16] A detailed description of the thermodynamic model was summarized by Rafal et al.[20] and Zemaitis et al.[21]

Prior to utilizing the thermodynamic model, we have selected the candidate starting materials for hydrothermal synthesis. Lead acetate and titanium oxide have been chosen as starting materials for the formation of $PbTiO_3$. TMAH ($C_4H_{12}NOH$) is used as a pH-adjusting agent. Subsequently, the thermodynamic model is used to predict the concentrations and activities of all aqueous species in the Pb–Ti–TMAH–H_2O system. For this purpose, standard-state properties of all chemical species (i.e., gaseous, charged and uncharged aqueous species and solid phases) in the hydrothermal system should be known. These properties include the standard Gibbs energy of formation $\Delta_f G^o$, enthalpy of formation $\Delta_f H^o$ and entropy S^o at a reference temperature (298.15 K) as well as partial molar volume V^o and heat capacity C_p^o as functions of temperature.

Thermochemical data for most of the species in the system of interest have been already published.[11,12] However, standard-state properties for $C_4H_{12}NOH$, tetramethylammonium ion ($C_4H_{12}N^+$) and a pyrochlore phase $Pb_2Ti_2O_6$ are not available in the literature and had to be estimated. The absolute entropy (S^o) of $C_4H_{12}N^+$ is given by Coulter et al.[22] The Gibbs energy ($\Delta_f G^o$) and enthalpy of formation ($\Delta_f H^o$) are calculated using solubility measurements for $C_4H_{12}NI$ and $C_4H_{12}NBr$ in water at 25 °C combined with auxiliary data.[23,24] The heat capacity and molar volume of $C_4H_{12}N^+$ are taken from Marcus.[25] Gibbs energy of formation for solid $C_4H_{12}NOH$ were estimated using a general relationship for the Gibbs free energy of formation of metal hydroxides developed by Sverjensky and Molling.[26] The same approach was used for the calculation of the enthalpy of formation for $C_4H_{12}NOH$. The heat capacity was estimated using a group contribution method.[27]

It is well known that a pyrochlore phase $Pb_2Ti_2O_6$ may form in the Pb–Ti-mineralizer hydrothermal system under certain conditions.[28] In particular, this may occur when hydrous TiO_2 is used as a precursor.[29] There might be other pyrochlores in this system as reported by Takai et al.[28] Unfortunately, we have no information at all about the stability and/or solubility of these or structurally similar phases in aqueous solution. Therefore, it was impossible to take them into account in our calculations because estimations would be too uncertain. Also, data for hydrous TiO_2 are not available in the literature. Therefore, validation of calculated yield diagrams may be a subject to some inherent limitations.

Repetitive application of the model for different input concentrations of lead acetate ($PbAc_2$) and TiO_2 as well

as $C_4H_{12}NOH$ makes it possible to construct stability and yield diagrams. A computer program has been developed for the automatic generation of these diagrams.[19] Stability diagrams show the ranges of equilibrium conditions for which lead titanate is stable in the hydrothermal system. Yield diagrams specify the reaction conditions required for an assumed yield of $PbTiO_3$. As the y-axis variable of yield diagrams, the program uses the input concentrations of lead acetate or/and titanium dioxide, which is equal to the initial concentration of the metal precursor. The ratios of the input precursor concentrations are held constant at a predetermined value. As the x-axis variable, the program can use either pH or the input concentration of a mineralizer. All concentrations are expressed in molalities because such units are easily measurable.

2.2. Yield diagrams of the Pb–Ti–$C_4H_{12}NOH$–H_2O system

Fig. 1 (A) shows the calculated yield of $PbTiO_3$ at 423 K when the ratio of lead acetate to titanium dioxide is equal to 1.0 (Pb/Ti = 1.0). In this figure, the input molalities of the titanium precursor are plotted against the molality of tetramethylammonium hydroxide. The lower solid line encompasses the region of stability of $PbTiO_3$. It determines the incipient precipitation line. It should be noted that the part of the incipient precipitation line that lies at low pH is not shown in Fig. 1(A) because it corresponds to acidic environments. Phase-pure lead titanate (yield above 99%) can form in a relatively narrow region of input precursor and mineralizer molalities that is shown as a shaded area in Fig. 1(A). In the region outside the 99% yield of $PbTiO_3$ but within the stability area of lead titanate (cf. the region between the solid line and the shaded area), a mixture of unreacted TiO_2 and $PbTiO_3$ is expected to form. In the vicinity of the shaded region, a relatively high yield of lead titanate is expected (e.g., 99%).

Fig. 1(B) shows a yield diagram for a system obtained by mixing $PbAc_2$ and TiO_2 with the ratio of Pb/Ti equal to 1.1. The calculations simulate the behavior of this system at 423 K with $C_4H_{12}NOH$ as

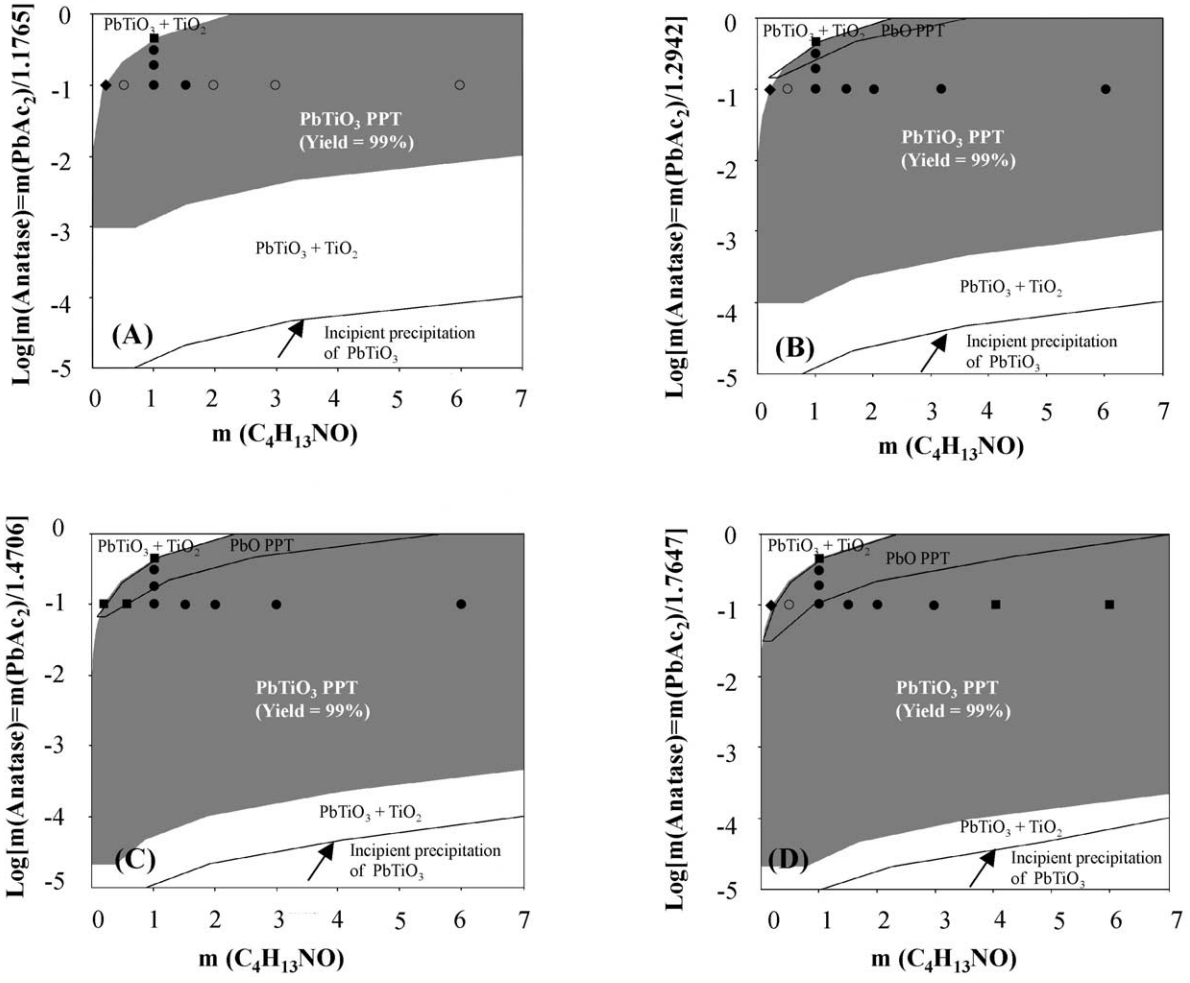

Fig. 1. A flow chart representing processing steps for the preparation of $PbTiO_3$ particles by hydrothermal method.

a mineralizer. The location of the incipient precipitation line is insensitive to the ratio of Pb/Ti in this system. This is consistent with our previous work[12] where KOH was used as a pH-adjusting agent. On the other hand, the area of the perovskite phase-purity region significantly widens when the ratio of Pb/Ti is greater than one. In particular, the area for which the yield of lead titanate is above 99% is very big as shown by the shaded region in Fig. 1(B). $PbTiO_3$ precipitates along with PbO in the small region shown at the top of the phase-purity region and encompassed by a solid line. The stability area of PbO is rather small and limited to high input concentration of lead precursor and $C_4H_{12}NOH$ concentration below 3 m. In highly alkaline solutions, lead oxide dissolves. Our calculations show that the maximum amount of $PbTiO_3$ contamination by PbO is equal to 8.4%. When the Pb/Ti ratio increases as shown in Fig. 1(C) and (D), the area of the yield of lead titanate above 99% widens by moving gradually toward the incipient precipitation line. Also, the area of PbO stability significantly increases. For example, for the Pb/Ti ratio equal to 1.5 it covers the range of $C_4H_{12}NOH$ concentrations up to 7 m and starts at TiO_2 concentration equal to 0.03 m as compared to 0.01 m for the Pb/Ti ratio equal to 1.1 as shown in Fig. 1(D).

3. Experimental procedure

The process to prepare $PbTiO_3$ particles by hydrothermal treatment is schematically illustrated in Fig. 2. Hydrothermal synthesis was performed using tetramethylammonium hydroxide pentahydrate, $C_4H_{12}NOH{\cdot}5H_2O$, (Aldrich Chemical, Milwaukee, WI, 97%) as a mineralizer. Throughout the process, the CO_2-free deionized water was used in the preparation of all the aqueous solution to prevent the contamination of lead basic carbonates. Lead acetate trihydrate, $Pb(CH_3COO)_2{\cdot}3H_2O$, (Fisher Scientific, Fair Lawn, NJ, 99%) was used as a source of Pb, and was used as received. The titanium hydrous gel, $TiO_2{\cdot}nH_2O$, was used as a source of Ti and was prepared by hydrolytic decomposition of titanium tetraisopropoxide as follows: ttitanium(IV) isotetrapropoxide (2.05 g) (Aldrich Chemical, Milwaukee, WI, 97%) was diluted with 100 ml 2-propanol (Fisher Scientific, Fair Lawn, NJ). A solution containing 10 ml CO_2-free deionized water (10 MΩ·cm, Millipore Corp., Bedford, MA) and 40 ml 2-propanol was used for hydrolytic decomposition. CO_2-free deionized water had been prepared by boiling for 15 minute under nitrogen gas. The hydrous oxide precursors were washed by repeated cycles of centrifugation (Induction Drive Centrifuge, Model J2-21M, Beckman Instruments, Inc., Palo Alto, CA) and redispersion in CO_2-free deionized water. Washing was performed for a minimum of two times in CO_2-free deionized water. Excess water was decanted after the final washing and the wet precursor was redispersed in a total volume 70 ml of CO_2-free deionized water (based on total water basis) under vigorous stirring. Lead acetate trihydrate and TMAH were then added in known quantity, respectively. Several modifications to the standard synthesis procedure were incorporated to study the influence of different synthesis conditions on phase composition and particle morphology. The concentation of reactants (i.e. $PbAc_2$) varied from 0.05 to 0.4 m. Reactions were carried out with a stoichiometric Pb/Ti ratio from 1 to 1.5 for wide range of solution pH. The concentration of TMAH varied from 0.5 to 6 m for the desired pH of the hydrothermal medium. The resulting suspension was placed in 110 ml stainless steel Telflon-lined autoclaves (Large Capacity Acid Digestion Bomb: Parr Instrument Co., Moline, IL) with a fill factor of 65%. The atmosphere inside the pressure vessel was flushed with nitrogen prior to sealing the autoclave heating contents to the desired temperature.

The reaction vessel was then heated to the desired temperature at a rate of 3 °C/min by a close-fitting insulated heating mantel (Glas-Col, Terre Haute, IN) placed on a hot plate and magnetically stirred. The reaction time at the desired temperature was varied from 1.5 to 96 h. Stirring was employed throughout the reaction unless mentioned otherwise. After hydrothermal treatment, the vessel was cooled in ambient air to ~40 °C prior to opening the autoclave. The solid reaction products were washed at least five times by repeated cycles of centrifugation and redispersion in ethanol.

After washing, the recovered powders were dried at 25 °C in a desiccator for 48 h. The dried, recovered powders were analyzed for phase composition using X-ray diffraction (Siemens D500 diffractometer: Siemens Analytical X-ray Instruments, Inc., Madison, WI) over the 2θ ranges from 4 to 90° with counting times of 3 s per 0.03° step. Identity of the phases present was determined by matching the experimental pattern with standards compiled by the Joint Committee on Powder Diffraction Standards. The morphologies of the synthesized particles were observed using advanced field-emission scanning electron microscopy (FESEM: LEO Electron Microscopy Inc, Thornwood, NY). Semiquantitative analyses of the platelet-like intermediate phase were carried out on a PGT (Princeton Gamma Tech, Princeton, NJ) digital energy dispersive spectroscopy (EDS) with position-tagged spectrometry (PTS), using an accelerating voltage ranging from 10 to 15 kV. Peak overlap of the titanium K_α and lead L_α lines was resolved by standardless multi-point analysis IMIX software.

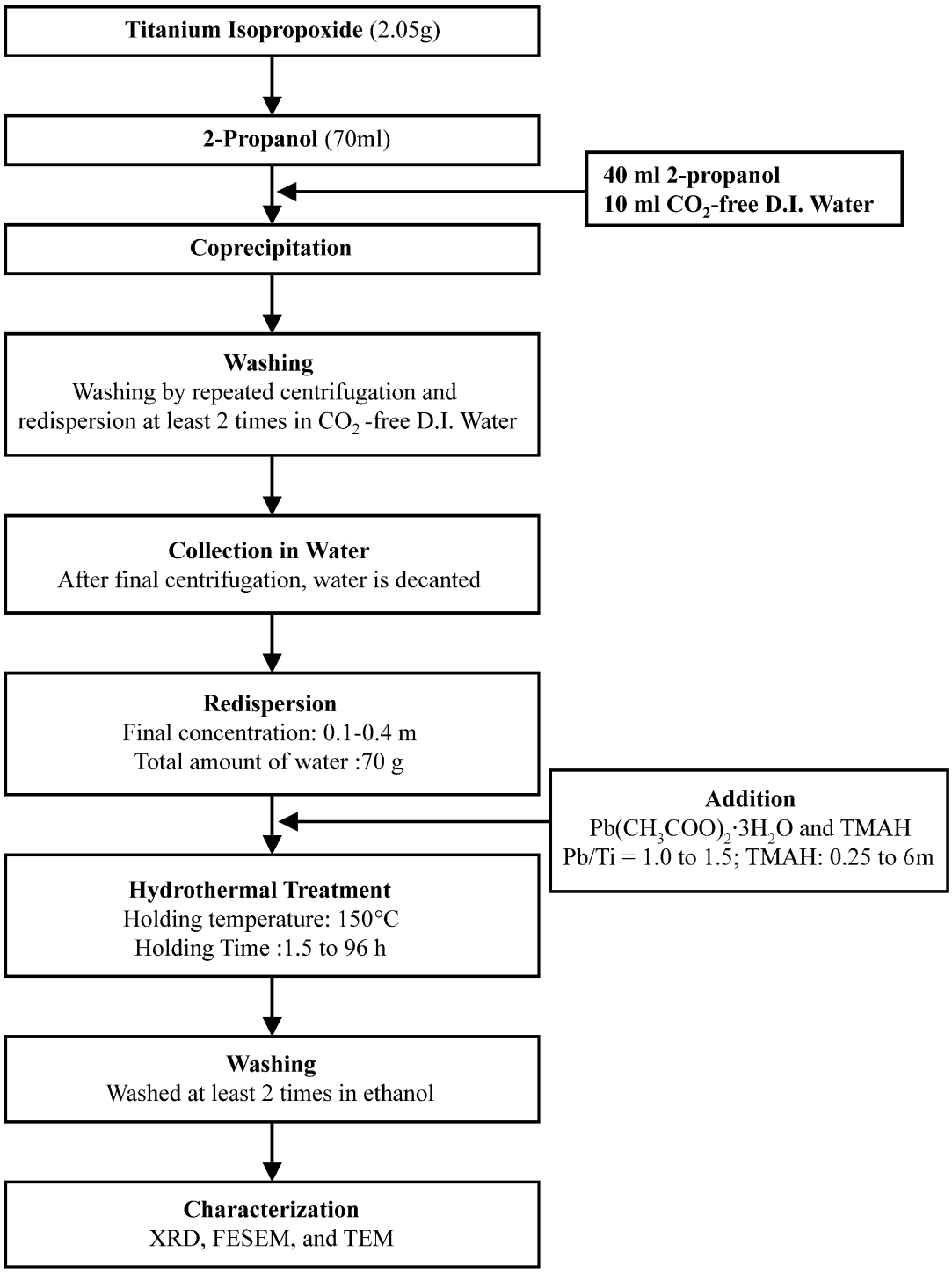

Fig. 2. Calculated yield diagram for the precipitation of $PbTiO_3$ in the Pb–Ti hydrothermal system at 150 °C (423 K) with tetramethylammoion hydroxide (TMAH) as a mineralizer: (A) Pb/Ti = 1, (B) Pb/Ti = 1.1, (C) Pb/Ti = 1.25, and (D) Pb/Ti = 1.5. $Pb(CH_3COO)_2$ and TiO_2 were used as starting materials for the calculations.

4. Synthesis results

4.1. Synthesis for stoichiometric Pb/Ti ratio (Pb/Ti = 1)

To verify the thermodynamic modeling, the synthesis from precipitated titanium hydrous gel ($TiO_2 \cdot nH_2O$) was performed for several points of yield diagrams. Phase-pure perovskite $PbTiO_3$ powders are synthesized in the range from 1 to 1.5 m TMAH concentration that is corroborated with predictions of the model [Fig. 1(A), ●]. A mixture of perovskite and pyrochlore phases is synthesized at 0.5 m TMAH concentration [Fig. 1(A),

○]. At this concentration, our calculations predicted that phase-pure perovskite $PbTiO_3$ would result. Therefore, this experimental result was not in agreement with predictions. The difference between predictions and experimental result may have been due to sluggish reaction kinetics at low concentration of TMAH (low solution pH). A mixture of perovskite, pyrochore, and small amount of TiO_2 (anatase) are synthesized at 0.25 m TMAH concentration [Fig. 1(A), ◆]. At this concentration, our calculations predicted that perovskite $PbTiO_3$ and TiO_2 would result. Therefore, this experimental result indicate that the phase transformation from pyrochlore to perovskite is not complete at the reaction time of 48 h at low TMAH concentration (TMAH $\leqslant$0.5 m) because of sluggish reaction kinetics. Since XRD analysis results of TiO_2 phase are consistent with our calculations, it is expected that the phase transformation from pyrochlore to perovskite $PbTiO_3$ will be complete at longer reaction time. At the TMAH concentration ranging from 2 to 6 m, a mixture of perovskite and pyrochlore phases is synthesized [Fig. 1(A), ○]. At this concentration range, our calculations predicted that phase-pure perovskite $PbTiO_3$ would result. Therefore, these experimental results were also not in agreement with our calculation. The difference between predictions and experimental result suggests that high solution pH increase the solubility of lead and promotes dissolution or decomposition of perovksite phase which leads to slow phase transfromation from pylochlore to persovskite at high concentration of TMAH. Fig. 1(A) also shows the effect of starting TiO_2 concentration on the final product synthesized at Pb/Ti = 1.0 and 1.5 m TMAH. Phase-pure perovskite $PbTiO_3$ powders are synthesized in the range of 0.1 to 0.3m metal concentrations as expected in yield diagram [Fig. 1(A), ●]. Increasing the metal concentration from 0.3 to 0.4 m produced a mixture of perovskitea and pyrochlore phase [(Fig. 1(A), ○]. At this concentration, our calculations predicted that perovskite $PbTiO_3$ would result. The difference between predictions and experimental results indicates that the phase transformation from pyrochlore to perovskite in boundary region is not complete at the reaction time of 48 h at high TiO_2 concentration (TiO_2 $\geqslant$0.4 m).

4.2. Synthesis for nonstoichiometric Pb/Ti ratio (Pb/Ti = 1.1)

Phase-pure PT powders are synthesized in the range from 1 to 6 m TMAH concentration that is corroborated with predictions of the model [Fig. 1(B), ●]. The X-ray diffraction pattern was characteristic of this phase (JCPDS Card No. 6-452). These results show that excess lead condition compensates the solubility increase of lead and prevent dissolution or decomposition of $PbTiO_3$ particles at high concentration of TMAH. Consequently, excess lead condition promotes the reaction kinetics and is more favorable for the preparation of phase-pure perovskite $PbTiO_3$ when TMAH is used as a mineralizer. A mixture of perovskite and pyrochlore phases is synthesized at 0.5 m TMAH concentration [Fig. 1(B), ○]). At this concentration, our calculations predicted that phase-pure perovskite $PbTiO_3$ would result. A mixture of perovskite, pyrochore, and small amount of TiO_2 (anatase) are synthesized at 0.25 m TMAH concentration [Fig. 1(B), ◆]). At this concentration, our calculations predicted that perovskite $PbTiO_3$ and TiO_2 would result. The difference between predictions and experimental results indicates that the phase transformation from pyrochlore to perovskite is not complete at the reaction time of 48 h at low TMAH concentration (TMAH $\leqslant$0.5 m) even with excess lead concentration because of sluggish reaction kinetics. Fig. 1(B) also shows the effect of starting TiO_2 concentration on the final product synthesized at Pb/Ti = 1.1 and 1.5 m TMAH. Phase-pure perovskite $PbTiO_3$ powders are synthesized in the range of 0.1 to 0.2 m metal concentrations as expected in yield diagram [Fig. 1(B), ●]. Increasing the metal concentration from 0.2 to 0.3 m produced phase-pure perovskite $PbTiO_3$ powders [Fig. 1(B), ●]. At this concentration, our calculations predicted that perovskite $PbTiO_3$ and PbO would result. The difference between predictions and experimental results indicates that experimental errors attributed to XRD methodologies, and hydrothermal experimentation, and the limitations of the thermodynamic modeling are important factors. As XRD methods are constrained by high detection limits (> 5 vol.%) and its inability to detect amorphous phases, XRD methods do not detect PbO that is synthesized below detection limits. There is high possibility that PbO is below the detection limits because the maximum amount of $PbTiO_3$ contamination by PbO is equal to 8.4% by our calculations. Errors related to the thermodynamic modeling could include the many limitations of the database used for the calculations discussed earlier. Increasing the metal concentration from 0.3 to 0.4 m produced a mixture of perovskite, pyrochlore and PbO. At 0.4 m metal concentration, our calculations predicted that perovskite $PbTiO_3$ and PbO would result. The difference between predictions and experimental results indicates that the phase transformation from pyrochlore to perovskite is not complete at the reaction time of 48 h even at high excess lead concentration because high metal concentration (TiO_2 $\geqslant$0.4 m) makes the reaction kinetics sluggish in boundary region.

4.3. Synthesis for nonstoichiometric Pb/Ti ratio (Pb/Ti = 1.25)

Phase-pure perovksite $PbTiO_3$ powders are synthesized in the range from 1 to 6 m TMAH concentration

that is corroborated with predictions of the model [Fig. 1(C), ●]. These results show that excess lead condition favors the formation of phase-pure perovskite PT powder by preventing dissolution or decomposition of $PbTiO_3$ particles at high concentration of TMAH. Consequently, excess lead condition promotes the reaction kinetics toward the synthesis of phase-pure perovskite $PbTiO_3$ when TMAH is used as a mineralizer. A mixture of perovskite, pyrochlore and PbO phases is synthesized below 0.5 m TMAH concentration [Fig. 1(C), ■]. Our calculations predicted that perovskite $PbTiO_3$ and PbO would result at 0.5 m TMAH concentration whereas our calculation at 0.25 m TMAH concentration is outside the region of $\geqslant$99% yield of perovskite $PbTiO_3$ and predicted that a mixture of $PbTiO_3$ and TiO_2 would result. The difference between predictions and experimental results indicates that the phase transformation from pyrochlore to perovskite is not complete at the reaction time of 48 h at low TMAH concentration (TMAH $\leqslant$0.5 m) even with excess lead concentration because the thermodynamic modeling could not predict the kinetic behavior such as sluggish reaction. The thermodynamic modeling could not also predict the precipitation of PbO at 0.25 m TMAH concentration because of the lack of thermochemical data. TMAH undergoes decomposition to trimethylamine, $(CH_3)_3N$, at temperatures above 150 °C.[30] The decomposition of TMAH could promote the precipitation of PbO particles (massicot, JCPDS Card No. 5-570) because the decomposition of TMAH decreased the solution pH and then the solubility of lead species. Themodynamic prediction in Pb–Ti–KOH system[12] is qualitatively very similar to themodynamic prediction in Pb–Ti–TMAH system. In this temperature range, themodynamic prediction in Pb–Ti–KOH system was fully corroborated by experimental results. Thus, both theory and experiments indicates it is possible to synthesize phase-pure $PbTiO_3$ using $PbAc_2$ and titanium hydrous oxide as precursors with the stoichiometric ratio Pb/Ti = 1.25 and pH = 11.8. Fig. 1(C) also shows the effect of starting TiO_2 concentration on the final product synthesized at Pb/Ti = 1.25 and 1.5 m TMAH. Phase-pure perovskite $PbTiO_3$ powders are synthesized in the range of 0.1 to 0.2 m metal concentrations as expected in yield diagram [Fig. 1(C), ●]. Increasing the metal concentration from 0.2 to 0.3 m produced phase-pure perovskite $PbTiO_3$ [Fig. 1(C), ●]. At this concentration, our calculations predicted that perovskite $PbTiO_3$ and PbO would result. As 0.3 m metal concentration was in the boundary region of PbO precipitation, amount of PbO synthesized in this region might be below the detection limits. Other results for Pb/Ti ratio = 1.25 is qualitatively very similar to the results for Pb/Ti ratio = 1.1.

4.4. Synthesis for nonstoichiometric Pb/Ti ratio (Pb/Ti = 1.5)

Phase-pure perovskite $PbTiO_3$ powders are synthesized in the range from 1 to 3 m TMAH concentration that is corroborated with predictions of the model [Fig. 1(d), ●] whereas a mixture of perovskite $PbTiO_3$ and PbO phases is synthesized above 0.3 m TMAH concentration [Fig. 1(d), ■]. These results show that even high excess lead condition (Pb/Ti = 1.5) favors the formation of phase-pure perovskite $PbTiO_3$ powder by preventing dissolution or decomposition of $PbTiO_3$ particles in the range of TMAH between 1 and 3 m whereas high TMAH concentration (TMAH $\geqslant$4 m) increases the supersaturation level of lead species and promote the precipitation of lead oxide. Consequently, high excess lead condition (Pb/Ti $\geqslant$1.5) promotes the synthesis of phase-pure perovskite $PbTiO_3$ at moderate TMAH concentration (1 m$\leqslant$TMAH $\leqslant$3 m). Other results for Pb/Ti ratio = 1.5 is qualitatively very similar to the results for Pb/Ti ratio = 1.25.

The results of this study indicate that theoretical predictions of synthesis condition using the thermodynamic modeling can be reconciled to the experimental results excerp the boundary region and high TMAH concentrations and it is possible to predict the synthesis conditions of phase-pure $PbTiO_3$ powder in the Pb–Ti–TMAH system.

5. Formation mechanisms

The reaction time plays an important role in the phase transformations from amorphous titanium hydrous gel to perovskite $PbTiO_3$. The effect of reaction time (1.5 – 12 h) was studied under the synthesis condition of 150 °C, 1.5 m TMAH for the formation of perovskite $PbTiO_3$ as a function of Pb/Ti ratio. In case of Pb/Ti ratio = 1.1, the XRD patterns and SEM of the powders synthesized at different hydrothermal reaction times are given in Figs. 3 and 4, respectively. Figs. 3(A) and 4(A) summarize the characteristics of titanium hydrous gel. The amorphous titanium hydrous gel exhibits a fine, porous network structure, which is believed to be infiltrated by water as shown in Fig. 3(A). The interconnected network structure was experimentally observed by both the large surface area obtained via a nitrogen adsorption technique ($\approx$300 m^2/g) and TEM photomicrographs of the precursor as shown in Fig. 4(B). The phase transformation from titanium hydrous gel with lead acetate to perovskite $PbTiO_3$ is almost complete at a reaction time of 12 h, as seen in Fig. 3(B)–(E). This conversion to phase-pure perovskite $PbTiO_3$ is illustrated in the SEM photomicrographs shown in Fig. 4(C)–(F). The phase transformation from titanium hydrous gel to perovskite $PbTiO_3$ very rapidly

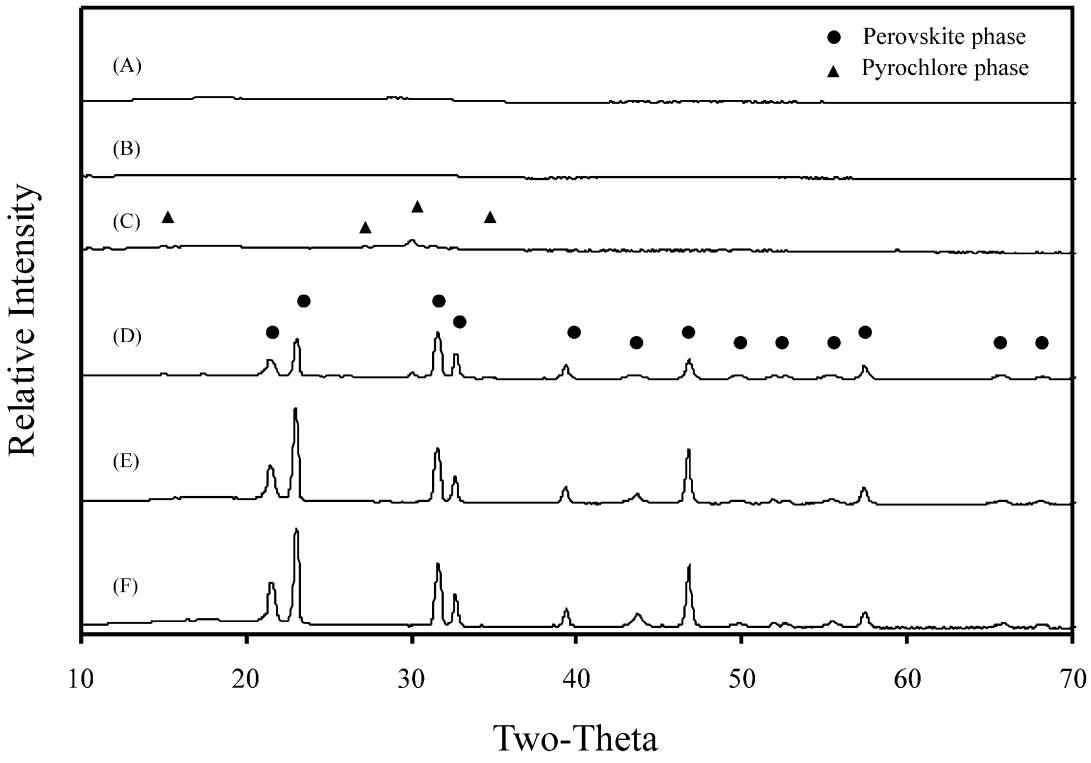

Fig. 3. XRD patterns showing the influence of the reaction time on the formation of cubic $PbTiO_3$ particles in hydrothermal condition (150 °C, 1.5 m TMAH, Pb\Ti = 1.1): (A) titanium hydrous gel precursor, (B) 1.5 h, (c) 3 h, (D) 6 h, (E) 12 h, and (F) 48 h.

occurs within 12 h as shown in Fig. 3(D) and (E). It was observed that pyrochlore phase appears at the early stage of reaction and the phase transformation from titanium hydrous gel to intermediate phase occurs with an induction period of 1.5 h as shown in Figs. 3(B) and 4(C). The reaction product at this stage primarily consists of submicron spherical pyrochlore phase (≈0.2–0.3 μm) and unreacted precursor. The phase transformation of precursor to intermediate pyrochlore phase is almost complete at a reaction time of 3 h as shown in Fig. 3(C). The phase transformation of intermediate pyrochlore phase to perovskite $PbTiO_3$ and subsequent growth of $PbTiO_3$ particles proceeds after the reaction time of 3 h and well developed $PbTiO_3$ particles (≈2–3 μm) formed at the reaction time of 6 h, as shown in Fig. 4(E). It is observed that the size of these PT particles increases from 2–3 to 4–5 μm at the reaction time of 12 h. After the reaction time is 12 h, there is no distinct morphology change of cubic $PbTiO_3$ particles and the intensity of XRD patterns slightly increased when the reaction time increased from 12 to 48 h as shown in Fig. 3(F).

In case of Pb/Ti = 1.25, the XRD patterns and SEM of the powders synthesized at different hydrothermal reaction times are given in Figs. 5 and 6, respectively. The nucleation and growth mechanism of $PbTiO_3$ particles at Pb/Ti = 1.25 is quite different from that at Pb/Ti = 1.1. The phase transformation from titanium hydrous gel to perovskite $PbTiO_3$ is almost complete at a reaction time of 12 h, as seen in Fig. 5(B)–(E). This conversion to phase-pure $PbTiO_3$ is illustrated in the SEM photomicrographs shown in Fig. 6(B)–(E). It was observed that two different platelet-like and spherical intermediate phase appears at the early stage of reaction and the phase transformation from titanium hydrous gel to pyrochlore intermediate phase occurs without induction period as shown in Figs. 5 (A) and 6(A). The reaction product at this stage primarily consists of platelet-like intermediate phase (≈5–10 μm) and spherical submicron intermediate phase (≈0.2–0.3 μm). The phase transformation of precursor to intermediate pyrochlore phases is almost complete at a reaction time of 1.5 h as shown in Fig. 5(A). The size of the intermediate platelet-like particles increased from 4–5 to 10–15 μm when the reaction time increased from 3 to 6 h as shown in Fig. 6(B) and (C). Finally, the intermediate platelet-like particles completely transform into phase-pure perovskite $PbTiO_3$ particles at the reaction time of 12 h. After the reaction time is 12 h, there is no distinct morphology change of platelet-like $PbTiO_3$ particles. The intensity of XRD patterns increased and thickness of platelet-like PT particles increased from 0.5 to 1 μm when the reaction time increased from 12 to 48 h as shown in Figs. 5(E) and 6(E).

To explain the reaction mechanism, a detailed structural investigation of the precursor and a study of crystallization kinetics are required. However, along with the supportive results of XRD and FESEM/PTS, a mechanism for the formation of the $PbTiO_3$ particles is

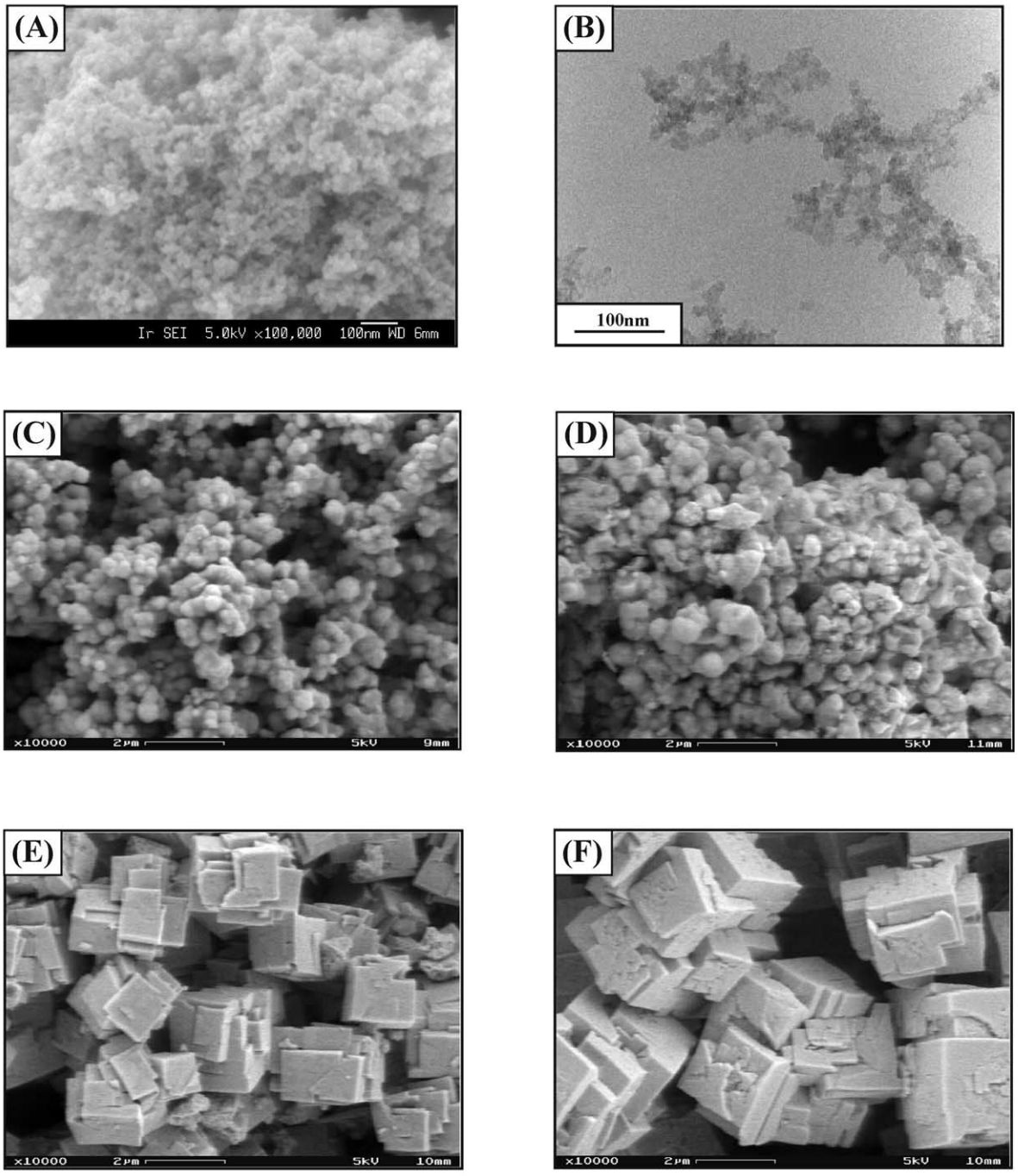

Fig. 4. SEM photomicrographs showing the influence of the reaction time on the formation of cubic $PbTiO_3$ particles in hydrothermal condition (150 °C, 1.5 m TMAH, Pb\Ti = 1.1): (A) titanium hydrous gel precursor, (B) TEM photomicrographs of titanium hydrous gel, (C) 1.5 h, (D) 3 h, (E) 6 h, and (F) 12 h.

believed to involve dissolution and recrystallization of poorly organized precursor into the cubic or platelet perovskite $PbTiO_3$. There are two different possible growth mechanisms of $PbTiO_3$ as a function of Pb/Ti ratio.

There are two main features that must be pointed out in the morphological characteristics of the different solid phases involved in the reaction. First, there is no similarity between the morphologies of the precursor materials, the intermediate phase and/or cubic or platelet $PbTiO_3$ particles. Second, the $PbTiO_3$ particles obtained at the end of the reaction exhibit a very narrow size distribution. The proposed reaction mechanism must account for these two primary features.

The different morphologies of the three solid phases involved in the system can only be explained if the transformation of one phase into another proceeds via the solution with dissolution and nucleation-growth

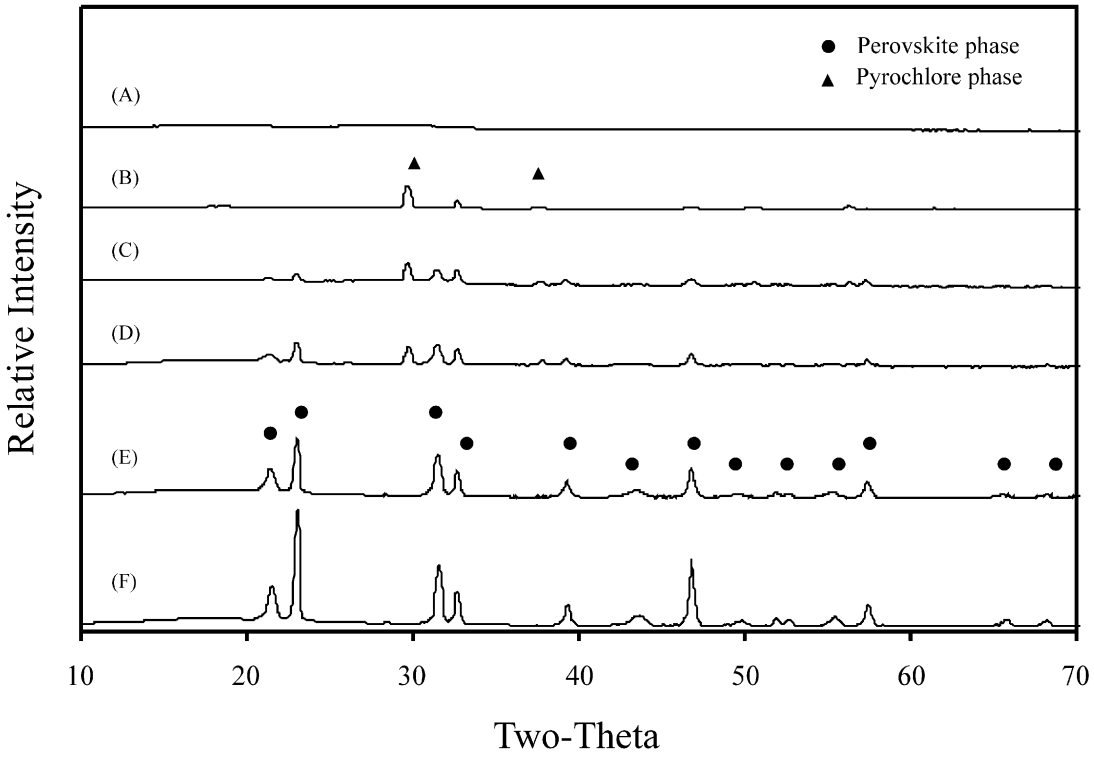

Fig. 5. XRD patterns showing the influence of the reaction time on the formation of platelet-like $PbTiO_3$ particles in hydrothermal condition (150 °C, 1.5 m TMAH, Pb\Ti = 1.25): (A) titanium hydrous gel precursor, (B) 1.5 h, (C) 3 h, (D) 6 h, (E) 12 h, and (F) 48 h.

steps. Therefore, the occurrence of an intermediate phase leads to the mechanism of reaction with two consecutive stages as described in Fig. 7. This mechanism must also account for the fact that the $PbTiO_3$ particles obtained is almost monodispersed. A condition that must be fulfilled in order to obtain such monodispersed particles is the separation of the nucleation and growth steps.[31,32] This condition has been expressed by Lamer and Dinegar[33] for the preparation of sulfur sol from acidified thiosulfate solutions. Alternatively, the generation of reacting species by the process generally known as Precipitation From Homogenous Solution (PFHS) is often observed in systems where temperature is used to thermally decompose precursor materials.[9,34] Rossetti et al.[9] reported, in such system that a sparingly soluble precursor hydrous oxide was used to generate the reacting species, a high yield of product powder is potentially attainable using relatively concentrated precursor suspensions. Furthermore, the high concentration of feedstock is not expected to compromise the generation of nuclei as it does in classical PFHS because the reservoir of nutrient stored in the solid precursor does not influence solution factors such as supersaturation and ionic strength.

Transport of Pb^{2+} solute species through the porous network structure is extremely rapid in comparison to bulk diffusion through a freshly formed $PbTiO_3$ product layer. Therefore, it is reasonable to assume that due to the relatively high solubility of Pb^{2+} ions with respect to the titanium species, the Pb^{2+} species cover the entire surface of the porous titanium hydroxide gel throughout the reaction.[35] Pb^{2+} species initially adsorbed on the gel surface are then incorporated into the gel. This causes the breaking of Ti–O–Ti bonds in the highly cross-linked hydrous gel and rearrangement accompanied by the dehydration of the gel. In this condition, it is believed that porous titanium hydrous precursor with Pb^{2+} species was transformed into intermediate pyrochlore phase and isothermal reaction of the amorphous titanium hydrous gel and Pb^{2+} species is limited by a local phase boundary chemical reaction in which the rate-controlling step entails a chemical reaction at the gel surface. Local nucleation and initial growth are marked by Pb^{2+} incorporation to the nuclei lattice. According to this scheme, in the case of Pb/Ti = 1.1, the structure of titanium hydrous gel rearranges with lead species by dissolution to form critical nuclei for spherical intermediate pyrochlore phase during the incubation time, then primary pyrochlore $PbTiO_3$ particles precipitate rapidly from a supersaturated solution at the early stage of the reaction as shown in Fig. 3(C). Supersaturation of perovskite cuboid $PbTiO_3$ is believed to slowly provide in the solution by gradual dissolution of the intermediate pyrochlore phase. Initially, the concentration of the reactants for the formation of cuboid perovskite $PbTiO_3$ in solution builds up till it reaches the saturation concentration. To obtain $PbTiO_3$ particles with narrow size distribution, spontaneous nucleation

occurs with the formation of many nuclei in a short time and these nuclei grow rapidly relative to the dissolution of the intermediate phase and consequently, the concentration of reactants is rapidly decreased below the critical supersautration for nucleation but remains higher than the saturation concentration for growth. The further growth of the particles continues at a rate that promotes consumption of all reactants generated by the dissolution reaction without any further nucleation. The final cuboid $PbTiO_3$ particles are thus obtained from the growth of these nuclei resulting in particles with a narrow size distribution and a uniform shape as shown in Fig. 4(F).

In the case of Pb/Ti = 1.25, the structure of titanium hydrous gel rearranges with excess lead species by dissolution to form two different intermediate phases at the early stage of the reaction; one is submicron spherical pyrochlore phase and the other is platelet pyrochlore phase. In our study, it is demonstrated that excess lead condition (Pb/Ti > 1.1) need to form the platelet intermediate phase

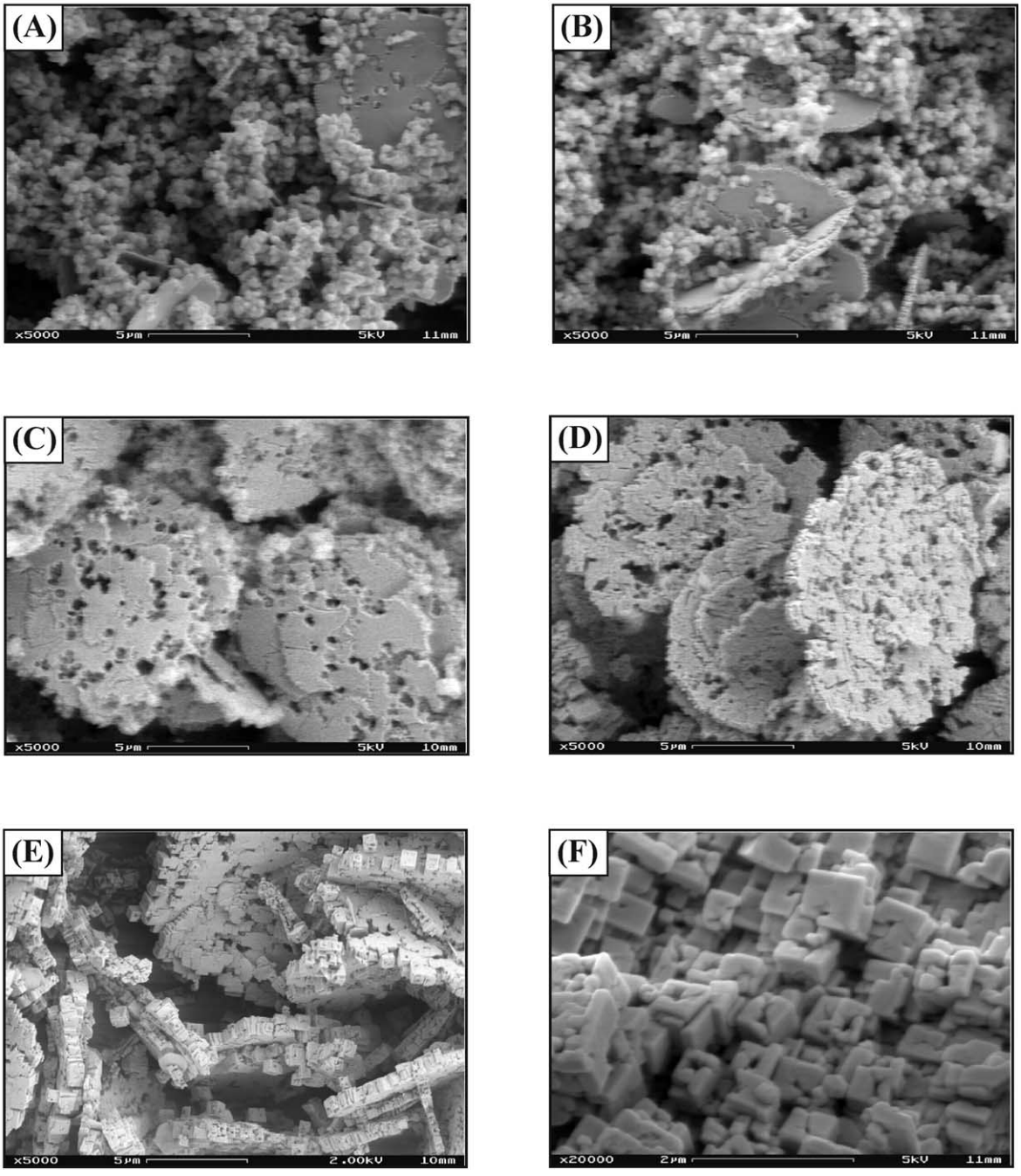

Fig. 6. SEM photomicrographs showing the influence of the reaction time on the formation of platelet-like $PbTiO_3$ particles in hydrothermal condition (150 °C, 1.5 m TMAH, Pb\Ti = 1.25): (A) 1.5 h, (B) 3 h, (C) 6 h, (D) 12 h, (E) 48 h, and (F) small cubes on $PbTiO_3$ platelet.

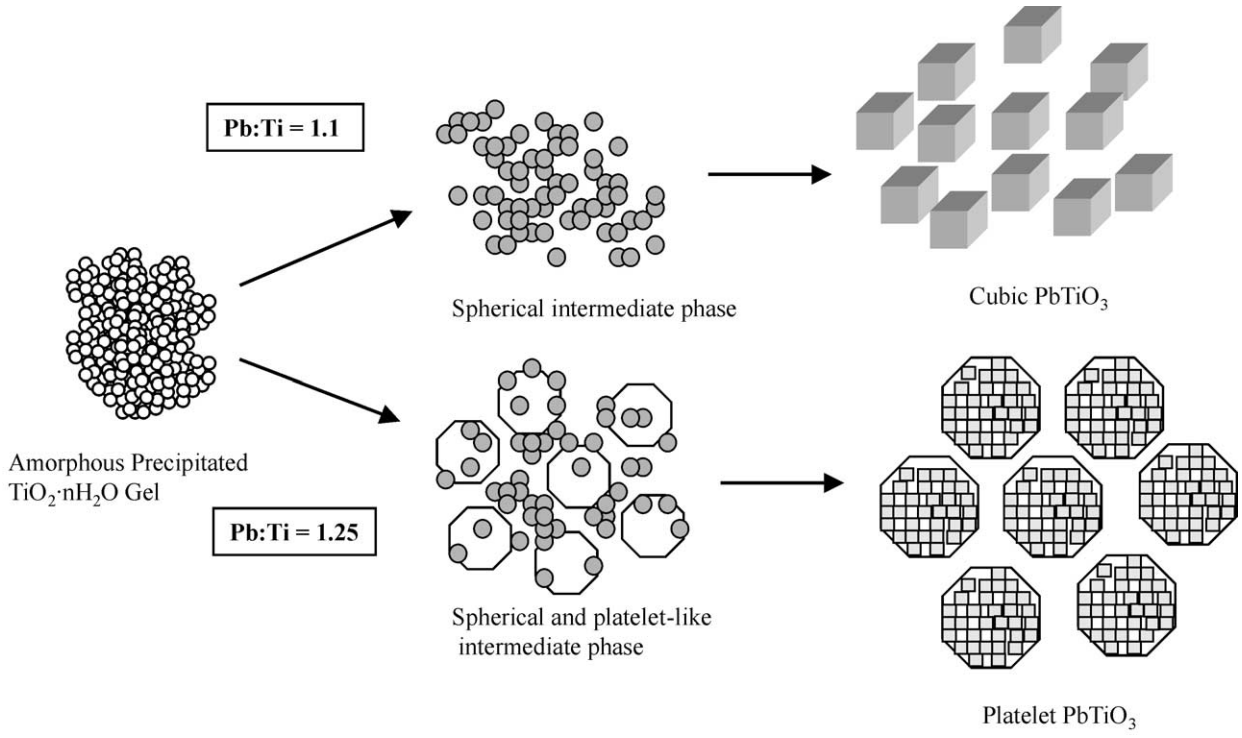

Fig. 7. Proposed $PbTiO_3$ particle formation mechanism under hydrothermal conditions using TMAH as an organic mineralizer.

in the reaction. The platelet-like intermediate phase is believed to be a PbO-rich solid solution in the PbO–TiO_2 system. It was shown by Cheng and coworkers[14] that the PbO-rich solid solution formed only when the reaction medium is above pH 14 and excess lead is present (Pb/Ti ratio <1.2). The solid solution particles have a tetragonal structure with a light yellow color and platelet shape. The composition was determined to be $PbTi_xO_{1+2x}$ where $x=0.80\pm0.02$. In our study, it is also demonstrated that platelet-like intermediate phase is a PbO-rich solid solution and its composition was determined to be $PbTi_xO_{4x}$ whtere $x=0.60\pm0.1$ by using multi-point analysis IMIX software. This platelet pyrochlore phase is believed to be thermodynamically more stable than spherical pyrochlore phase in high solution pH condition because the intermediate platelet-like PbO-rich solid solution grew from 4–5 to 10–15 μm with consumption of spherical pyrocholre phases when the reaction time increased from 3 to 6 h. Supersaturation of perovskite $PbTiO_3$ is slowly provided in the solution by gradual dissolution of the intermediate spherical pyrochlore phase. Initially, the concentration of the reactants for the formation of cuboid $PbTiO_3$ in solution builds up till it reaches the saturation concentration. Platelet intermediate particles acts as a template to preserve the platelet shape in final product and small cubic shape $PbTiO_3$ grains grew on the surface of these platelets and the thickness of these platelet particles gradually increased during further hydrothermal treatment as shown in Fig. 6 (D) and (E). The further growth of platelet particles continues at a rate that promotes consumption of all reactants generated by the dissolution reaction without any further nucleation. It is also observed that small cubic shape $PbTiO_3$ grains on the surface of platelets also have much more distinct shape when the reaction time increased as shown in Fig. 6(F). The final platelet $PbTiO_3$ particles have a narrow size distribution and a uniform shape as shown in Fig. 6(E).

These growth mechanisms suggest that the crystal growth of $PbTiO_3$ particles, which follows crystal nucleation, can be changed by either the availability of precipitating ions around the growing particles or by their subsequent binding to the particle surface simply depending on the Pb/Ti ratio.

6. Conclusion

Electrolyte thermodynamics made it possible to determine the optimum condtion (pH, concentration, Pb/Ti ratio) for the synthesis of crystalline $PbTiO_3$ from simple precursors such as lead acetate and titanium hydrous oxide. Also, it clarified the conidtions that are undesirable for the synthesis because $PbTiO_3$ is either unstable or contaminated with other solids.

Morphological evolution as a function of reaction time and the existence of fibrous intermediate phase implies that the particles formation mechanism of $PbTiO_3$ in the Pb–Ti–TMAH–H_2O system is dissolution and reprecipitation and there are two different particle

growth mechanisms depending on Pb/Ti ratio. PT particles have cubic shape in the case of Pb/Ti = 1.1 whereas platelet PT particles grew on platelet intermediate phase in the case of Pb/Ti = 1.25.

References

1. Johnson Jr., W., Innovations in ceramic powder preparation. In *Advances in Ceramics, Vol. 21, Ceramic Powder Science*, ed. G. L. Messing, K. S. Mazdiyasni, J. W. McCauley and R. A. Haber. The American Ceramic Society Inc, Westerville, OH, 1987, pp. 3–19.
2. Matijevic, E., Preparation and properties of uniform size colloids. *Chem. Mater.*, 1993, **5**, 412–426.
3. Dawson, W. J., Hydrothermal synthesis of advanced ceramic powders. *Am. Ceram. Soc. Bull.*, 1989, **67**(10), 1673–1678.
4. Jaffe, W., Cook Jr., R. and Jaffe, H., *Piezoelectric Ceramics*. Academic Press, New York, 1971.
5. Shrout, T. R., Papet, P., Kim, S. and Lee, G-H., Conventionally prepared submicrometer lead based perovskite powders by reactive calcination. *J. Am. Ceram. Soc.*, 1990, **73**(7), 1862–1867.
6. Blum, J. B. and Gurkovich, S. R., Sol-gel derived $PbTiO_3$. *J. Mater. Sci.*, 1985, **20**, 4479–4483.
7. Kim, M. J. and Matijevic, E., Preparation and characterization of uniform submicrometer lead titanate particle. *Chem. Mater.*, 1989, **1**, 363–369.
8. Fox, G. R., Adair, J. H. and Newnham, R. E., Effect of pH and H_2O_2 upon coprecipitated $PbTiO_3$ powders: Part I properties of as-precipitated powders. *J. Mater. Sci.*, 1990, **25**, 3634–3640.
9. Rossetti, G. A. Jr., Watson, D. J., Newnham, R. E. and Adair, J. H., Kinetics of the hydrothermal crystallization of the perovskite lead titanate. *J. Cryst. Growth*, 1992, **116**, 251–259.
10. Cheng, H., Ma, J., Zhao, Z., Qiang, D., Li, Y. and Yao, X., Hydrothermal synthesis of acicular lead titanate fine powders. *J. Am. Ceram. Soc.*, 1992, **75**(5), 1123–1128.
11. Lencka, M. M. and Riman, R. E., Thermodynamic modeling of hydrothermal synthesis of ceramic powders. *Chem. Mater.*, 1993, **5**, 61–70.
12. Lencka, M. M. and Riman, R. E., Synthesis of lead titanate: thermodynamic modeling and experimental verification. *J. Am. Ceram. Soc.*, 1993, **76**(10), 2649–2659.
13. Ohara, Y., Koumoto, K., Shimizu, T. and Yanagida, H., Hydrothermal synthesis of fibrous lead titanate powder. *J. Ceram. Soc. Jpn*, 1994, **102**, 88–92.
14. Cheng, H., Ma, J. and Zhao, Z., Hydrothermal synthesis of PbO–TiO_2 solid solution. *Chem. Mater.*, 1994, **6**(7), 1033–1040.
15. Jooho, M., Li, T., Randall, C. A. and Adair, J. H., Low temperature synthesis of lead titanate by a hydrothermal method. *J. Mater. Res.*, 1997, **12**(1), 189–197.
16. Gersten, B., Lencka, M. and Riman, E., Engineered low temperature hydrothermal synthesis of phase-pure lead-based perovskites using ethylenediamine tetra-acetic acid complexation. *Chem. Mater.*, 2002, **14**, 1950–1960.
17. Beal, K. C., Precipitation of lead zrconate titanate solid solution under hydrothermal conditions. In *Advances in Ceramics, Vol. 21, Ceramic Powder Science*, ed. G. L. Messing, K. S. Mazdiyasni, J. W. McCauley and R. A. Haber. The American Ceramic Society Inc, Westerville, OH, 1987, pp. 33–41.
18. Riman, R. E., Lencka, M. M., McCandlish, L. E., Gersten, B. L., Anderko, A., and Cho, S. B., Intelligent engineering of hydrothermal reactions. In *Proceedings of the Second International Conference on Solvothermal Reactions*, Takamatsu, Japan, December 1996, pp. 148–151.
19. *Environmental and Corrosion Simulation Programs (ESP/CSP)*. OLI Systems, Inc, Morris Plains, NJ, 1996.
20. Rafal, M., Berthold, J. W., Scrivner, N. C. and Grise, S. L., Models for electrolyte solutions. In *Models for Thermodynamic and Phase Equilibria Calculations*, ed. S. I. Sandler and M. Dekker. 601-670, New York, 1995.
21. Zemaitis, J. F. Jr., Clark, D. M., Rafal, M. and Scrivner, N. C., *Handbook of Aqueous Electrolyte Thermodynamics: Theory & Application*. AIChE, New York, 1986.
22. Coulter, L. V., Pitzer, K. S. and Latimer, W. M., The entropies of large ions; the heat capacity, entropy and heat of solution of potassium chloroplatinate, tetramethylammonium iodide and uranyl nitrate hexahydrate. *J. Am. Chem. Soc.*, 1940, **62**, 2845–2850.
23. Levien, B. J., Some physical properties of aqueous solutions of tetramethylammonium bromide and tetramethylammonium iodide. *Aust. J. Chem.*, 1965, **18**, 1161–1170.
24. Krivtsov, N. V., Titova, K. V. and Rosolovskii, V. Y., Enthalpy of formation of the hydrated $N(CH_3)_4^+$ ion and of certain tetramethylammonium salts. *Russ. J. Inorg. Chem.*, 1976, **21**(5), 769–770.
25. Marcus, Y., *Ion Solvation*. John Wiley & Sons Ltd, Chichester, England, 1985.
26. Sverjensky, D. A. and Molling, P. A., A linear free energy relationship for crystalline solids and aqueous ions. *Nature*, 1992, **356**, 231–234.
27. Kubaschewski, O. and Unal, H., An empirical estimation of the heat capacities of inorganic compounds. *High Temperatures-High Pressures*, 1977, **9**, 361–365.
28. Takai, K., Shoji, S., Naito, H. and Sawaoka, A., Fine powder $PbTiO_3$ obtained by hydrothermal technique and its sinterability. In *Proceedings of the First International Symposium on Hydrothermal Reactions*, ed. S. Somiya. 877-885, Tokyo, Japan, 1982.
29. Lencka, M. M., unpublished data.
30. *The Merck Index, An Encyclopedia of Chemicals, Drugs, and Biologicals*, 11th edn., ed. S. Budavari, Merck & Co., Inc., Rahway, NJ, 1989.
31. Overbeek, J. T. G., Monodisperse colloidal systems, fascinating and useful. *Advan. Colloid Interface Sci.*, 1982, **15**, 251–275.
32. Sugimoto, T., Preparation of monodispersed colloidal particles. *Advan. Colloid. Interface Sci.*, 1987, **28**, 65–108.
33. La Mer, V. K. and Dinegar, R. H., Theory, production and mechanism of formation of monodispersed hydrosols. *J. Am. Chem. Soc.*, 1950, **72**, 4847–4854.
34. Gordan, L., Salutsky, M. L. and Willard, H. H., *Precipitation from Homogeneous Solution*. Wiley, New York, NY, 1959.
35. Kutty, T. and Padmini, P., Wet chemical formation of nanoparticles of binary perovskites through isothermal gel to crystalline conversion. *Mater. Res. Bull*, 1992, **27**, 945–952.